

# Current Biology

## Transcriptional Pre-patterning of *Drosophila* Gastrulation

### Highlights

- T48/Fog pathway is prepatterned by localized transcription in the pre-cellular embryo
- Defined enhancers control the timing of gene activation in the premesoderm
- Differential transcriptional dynamics produce spatial gradients of *t48/fog* expression

### Authors

Bomyi Lim, Michael Levine,  
Yuji Yamazaki

### Correspondence

msl2@princeton.edu (M.L.),  
yujiy@princeton.edu (Y.Y.)

### In Brief

Lim et al. demonstrate that two key cellular effectors of mesoderm invagination, *t48* and *fog*, exhibit dynamic temporal changes in de novo transcription in response to the Dorsal morphogen gradient. These are likely to contribute to the graded distribution of myosin accumulation in the mesoderm prior to the onset of ventral furrow formation.



# Transcriptional Pre-patterning of *Drosophila* Gastrulation

Bomyi Lim,<sup>1</sup> Michael Levine,<sup>1,2,\*</sup> and Yuji Yamazaki<sup>1,3,\*</sup>

<sup>1</sup>Lewis-Sigler Institute for Integrative Genomics, Princeton University, Princeton, NJ 08544, USA

<sup>2</sup>Department of Molecular Biology, Princeton University, Princeton, NJ 08544, USA

<sup>3</sup>Lead Contact

\*Correspondence: [msl2@princeton.edu](mailto:msl2@princeton.edu) (M.L.), [yujy@princeton.edu](mailto:yujy@princeton.edu) (Y.Y.)

<http://dx.doi.org/10.1016/j.cub.2016.11.047>

## SUMMARY

Gastrulation of the *Drosophila* embryo is one of the most intensively studied morphogenetic processes in animal development [1–4]. Particular efforts have focused on the formation of the ventral furrow, whereby ~1,000 presumptive mesoderm cells exhibit coordinated apical constrictions that mediate invagination [5, 6]. Apical constriction depends on a Rho GTPase signaling pathway (T48/Fog) that is deployed by the developmental regulatory genes *twist* and *snail* [7–10]. It is thought that coordinate mesoderm constriction depends on high levels of myosin along the ventral midline, although the basis for this localization is uncertain. Here, we employ newly developed quantitative imaging methods to visualize the transcriptional dynamics of two key components of the Rho signaling pathway in living embryos, T48 and Fog. Both genes display dorsoventral (DV) gradients of expression due to differential timing of transcription activation. Transcription begins as a narrow stripe of two or three cells along the ventral midline, followed by progressive expansions into more lateral regions. Quantitative image analyses suggest that these temporal gradients produce differential spatial accumulations of *t48* and *fog* mRNAs along the DV axis, similar to the distribution of myosin activity. We therefore propose that the transcriptional dynamics of *t48* and *fog* expression foreshadow the coordinated invagination of the mesoderm at the onset of gastrulation.

## RESULTS AND DISCUSSION

Gastrulation is triggered by apical constrictions of myosin cables along the ventral midline of cellularized embryos. This localized activation of myosin depends on induction of Rho GTPases by T48 and the Fog/Mist GPCR signaling pathway (Figure 1A) [7, 8, 11]. T48, Fog, and Mist are each regulated by different combinations of the Dorsal, Twist, Snail regulatory network that controls dorsal-ventral patterning of the early embryo (Figure 1A) [7–9]. There is a loss of constrictions in mutants that

disrupt this pathway [11]. T48 is a transmembrane protein that directly binds RhoGEF2, leading to its recruitment to apical regions of individual mesoderm cells [7]. Fog is a ligand for Mist, a G-coupled receptor that induces Rho activation [9]. These two independent cellular effectors coordinate the apical constriction of mesoderm cells (Figure 1A). It is uncertain how dorsal-ventral regulatory determinants ultimately lead to restricted Rho signaling and myosin activation along the ventral midline because they are broadly expressed throughout the presumptive mesoderm.

Here, we employ newly developed quantitative imaging methods to visualize and measure the transcriptional dynamics of *t48* and *fog* expression in living *Drosophila* embryos [12, 13]. Conventional in situ hybridization assays revealed restricted expression of *t48* transcripts within the mesoderm, as well as an expansion of expression in the lateral ectoderm during later stages of development (Figure S1A). The mesoderm pattern of expression is two or three cells narrower than the Twist and Snail patterns, thereby raising the possibility of a subdomain within the mesoderm where apical constrictions are initially restricted [8, 14]. To determine how this functional subdomain is established, we sought to identify a mesoderm-specific *t48* enhancer. A few different putative enhancers were identified based on whole-genome Zelda chromatin immunoprecipitation sequencing (ChIP-seq) datasets [15, 16]. Each of the putative enhancers was cloned into a MS2/*yellow* reporter gene, which contains the minimal *eve* promoter and 24xMS2 RNA stem-loop repeats upstream of the ATG-start codon. One of the newly identified enhancers (int1 ENH) was found to recapitulate the endogenous *t48* expression pattern within the presumptive mesoderm (Figure S1B).

Nascent transcripts produced by the *t48*>MS2/*yellow* reporter gene were visualized as fluorescent foci using a maternally expressed MCP::GFP fusion protein. The intensities of these dots were measured over time to determine the transcriptional dynamics and cumulative outputs for each nucleus. Particular efforts focused on the first 20 min of nuclear cycle 14 (nc14) in order to capture the initial transcriptional dynamics of *t48* expression (Movie S1). At the midpoint of nc14 (~20–30 min following mitosis) the *t48* transcription pattern encompasses 10–14 cells across the ventral midline, which agrees with previous in situ hybridization assays. The first nascent transcripts appeared in posterior regions of the ventral midline within 5 min after mitosis. During the next 5 min, *t48* transcripts stochastically appeared as a narrow stripe of two or three cells in width along the anterior-posterior

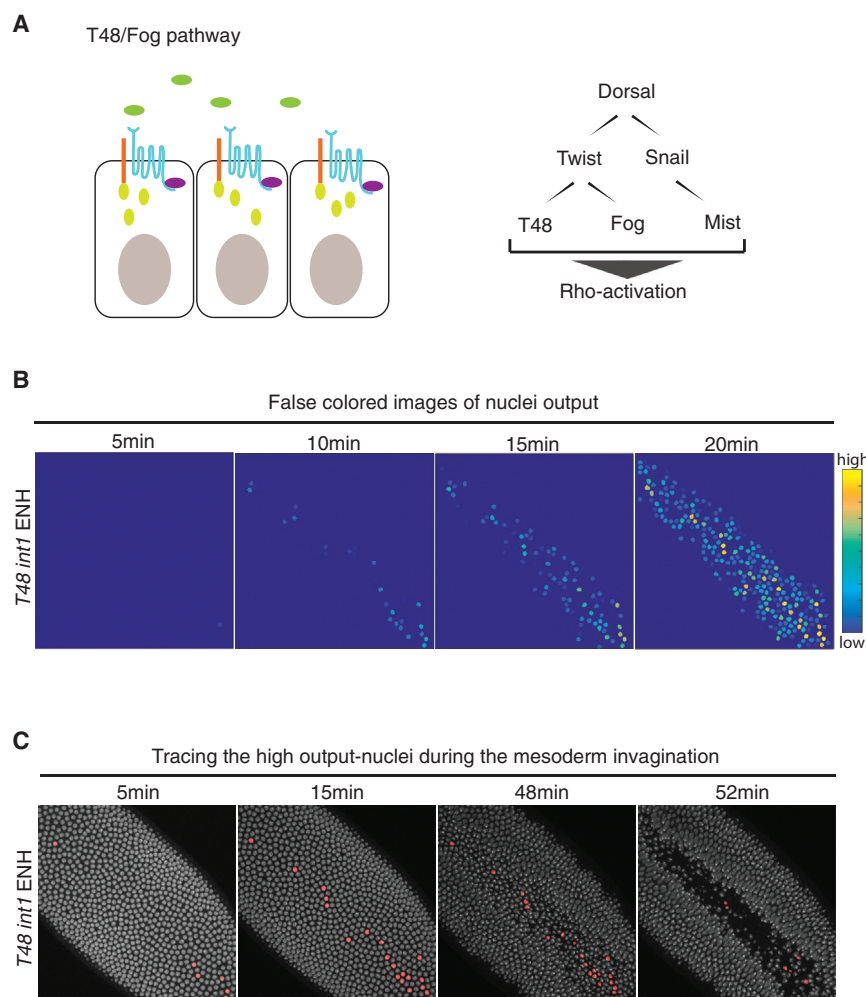


**Figure 1. T48/Fog Pathway and the Spatio-temporal Dynamics of *t48* Transcription in the Mesoderm**

(A) Schematic of *t48/fog* pathway during ventral furrow formation. Left: T48 (orange) and Mist (light blue) are apically localized. T48 recruits RhoGEF2 (yellow). Mist is a GPCR that interacts with concertina (purple). Fog ligands (green) are apically secreted. Fog/Mist activates Rho GTPase through RhoGEF2. T48/Fog pathway cooperatively activates Rho signaling. Right: maternal Dorsal activates Twist and Snail, and Twist activates *t48* and *fog*. *mist* is thought to be regulated by Snail. (B) Heatmap of cumulative output for *t48*-MS2/*yellow* transcripts during the first 20 min of nc14. (C) Twenty nuclei that produced the highest levels of *t48* transcripts during the first 20 min of nc14 were traced to mesoderm invagination. See also Figures S1 and S2 and Movie S1.

time point, suggesting minimal spatial variation among actively transcribing nuclei (Figures 2B and S2B). However, expression expands significantly over time, and to measure these dynamics, we divided nuclei into three groups based on their levels of cumulative RNA output (Figure 2C). We found that nuclei with the highest output are localized along the ventral midline, corresponding to those exhibiting earliest expression. Indeed, there is a statistically significant correlation between the timing of activation and cumulative output (Pearson's correlation coefficient =  $-0.70$ ; Figure 2D). Hence, the average cumulative RNA

outputs are graded along DV axis due to the timing in the onset of *t48* transcription (Figure 2E). We propose that this temporal gradient could contribute to the coordinated invagination of the mesoderm at later stages of development (see below).

*fog* is another critical component of the Rho signaling pathway controlling myosin activity during mesoderm invagination [8, 10]. *fog* and *mist* encode a ligand and receptor, respectively, of the GPCR pathway that induces Rho activity [9, 17]. Both genes are expressed in the presumptive mesoderm of pre-cellular embryos. We used CRISPR recombination to insert 24xMS2 stem loops into the 3' coding region of the endogenous *fog* locus [18] (Figure S1C). The transgenic flies carry a partial deletion of the *fog* coding sequence and, consequently, produce homozygous lethal embryos. Altogether, an  $\sim 9.5$ -kb cassette was inserted into *fog*, including the MS2 stem loops, a dsRed marker gene, and SV40 termination signals, including plasmid vector sequences. Because *fog* is a large gene ( $\sim 30$  kb in length), there is a delay in the detection of nascent transcripts as compared with the *t48*-MS2/*yellow* reporter gene containing 5' stem loops. Indeed, *fog*-MS2 signals were first detected in the mesoderm  $\sim 25$  min after the onset of nc14 (Figure 3A; Movie S2). Sporadic lateral MS2 signals were detected

(AP) axis. The transcription profile expands to 10–14 cells during the next 10 min (Figures 1B and 2A). The initial expression profile is interesting because this is the first indication of localized activity along the ventral midline of pre-cellular embryos (Figure S1A) [7]. We defined the cumulative RNA output of a given nucleus as the area under the transcription trajectory over time. Cumulative RNA outputs are graded along the dorsoventral (DV) axis during the first 20 min of nc14, reflecting the differential timing of *t48* transcription activation. The nuclei exhibiting the highest cumulative mRNA levels are located along the ventral midline (Figure 1B). To visualize this, we computationally labeled the 20 most highly expressed nuclei and traced them during mesoderm invagination (Figure 1C). These cells are indeed aligned along the midline of the ventral furrow, suggesting that the ventral midline is already established during the first 20 min of nc14.

To determine the basis for the graded distribution of *t48* transcripts, we measured the average fluorescent MS2 intensities along the DV axis during different time points. The boundaries between active and inactive nuclei expand progressively into ventro-lateral regions (Figures 2A and S2A; Movie S1). Transcription activity is reasonably constant at a given

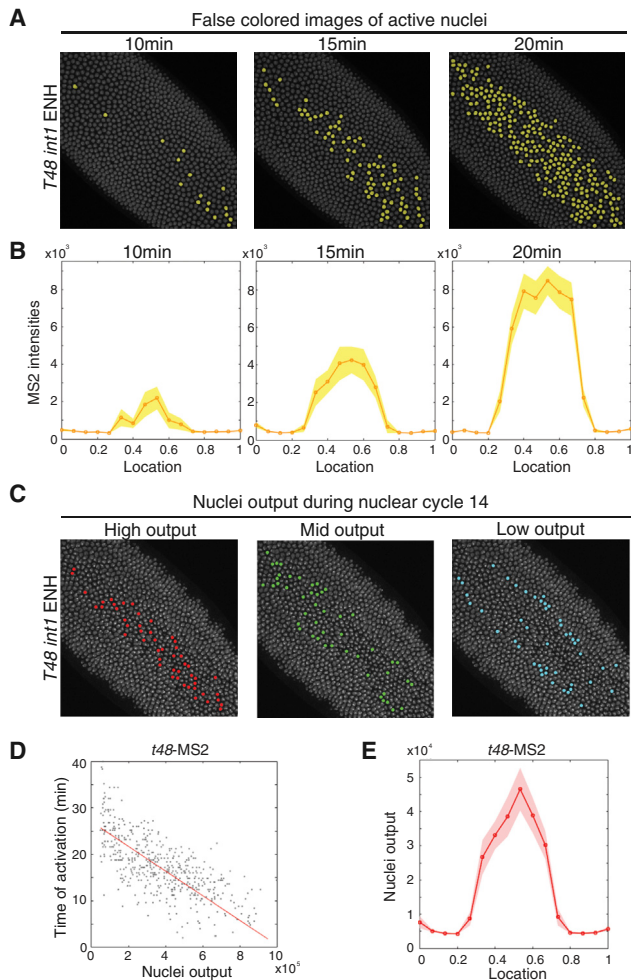


**Figure 2. Quantitative Analysis of *t48* Transcripts during Nuclear Cycle 14**

(A) Snapshots from a live imaging movie of an embryo expressing the *t48>MS2-yellow* transgene. Actively transcribing nuclei are false colored in yellow.

(B) Mean signal intensity of *t48>MS2* along the DV axis at each time point after the onset of nc14.

(C) Nuclei with high (90<sup>th</sup> percentile), middle (50<sup>th</sup> percentile), and low (10<sup>th</sup> percentile) output were colored in red, green, and cyan, respectively.

(D) Correlation between the timing of *t48*-transcriptional activation and cumulative RNA output during nc14. The Pearson correlation coefficient  $r = -0.70$  indicates a strong likelihood that differential expression is due to the timing of activation.

(E) Mean cumulative output of *t48>MS2* along the DV axis.

Shaded areas in (B) and (E) indicate the SEM of the nuclei along the same DV plane, and  $x = 0.5$  indicates the ventral midline. See also [Figures S1](#) and [S2](#) and [Movie S1](#).

earlier, and these might arise from a shorter transcript variant that is only 10 kb in length ([Figure S1C](#)).

As seen for *t48*, the first nuclei to exhibit *fog* nascent transcripts are located along the ventral midline. During the next 25 min, *fog* transcription expands laterally to a width of 12–15 cells ([Figures 3A](#) and [S3B](#)). The levels of transcription were measured at different time points across the DV axis ([Figure 3B](#)). *fog* transcription is initially detected in central mesoderm cells,

but there are similar levels of transcription along the DV axis at later stages. However, nuclei located near the lateral boundaries appear to possess weaker intensities due to stochastic, salt-and-pepper expression patterns ([Figure 3B](#)). The total levels of cumulative *fog* transcripts are graded along the DV axis, with higher output nuclei located in more ventral regions ([Figures 3C](#) and [3D](#)). There is a statistically significant correlation between the timing of activation and total RNA output (Pearson's correlation coefficient =  $-0.72$ ; [Figure S3A](#)). Thus, as seen for *t48*, there is a temporal gradient of *fog* expression that correlates with the gradient of myosin activity seen at the onset of mesoderm invagination (see [Figure 4B](#)). These gradients are due to the timing of transcriptional activation, rather than differential expression profile. Indeed, there is little difference in the maximum intensities of *t48* and *fog* transcripts along the DV axis at the midpoint of nc14 ([Figures 2B](#) and [3B](#)).

Fog ligands bind to at least two different receptors in early embryos, Mist and Smog [9, 17]. *mist* is zygotically expressed in the mesoderm and presumptive midgut, whereas *smog* is maternally deposited and uniformly expressed. Using Zelda ChIP-seq datasets, we identified a 2.1 kb genomic DNA that recapitulates the *mist* expression pattern in both the mesoderm and presumptive midgut ([Figure S1D](#)). Sporadic and ubiquitous expression of the *mist>MS2/yellow* reporter was detected prior to nc14 ([Movie S3](#)). These transcripts were also detected by in situ hybridization using an intronic probe (data not shown). After the onset of nc14, *mist* transcripts are detected in the mesoderm, along with a brief pulse of transcription in the lateral ectoderm. Quantitative analysis of the MS2 signals does not reveal a DV gradient of activity, as seen for *t48* and *fog* ([Figures 3E](#) and [S3C](#)). Instead, the *mist>MS2/yellow* reporter gene exhibits rapid and broad expression throughout the mesoderm, with slightly higher levels in anterior and posterior regions near the future sites of midgut invagination ([Figure 3F](#)). The correlation between the timing of activation and the total output of expression is weak (Pearson's correlation coefficient =  $-0.41$ ; [Figure 3G](#)). These observations are consistent with a variety of developmental processes (e.g., wing patterning in *Drosophila* and limb patterning in vertebrates), whereby broadly distributed receptors are controlled by spatially localized ligands [19, 20].

We have shown that two key signaling components of myosin activity, *t48* and *fog*, exhibit temporal gradients of expression at least 30 min prior to the onset of gastrulation. These gradients tightly mirror the distribution of myosin activity that mediates coordinated apical constrictions and invagination of the mesoderm ([Figure 4](#)). These gradients do not arise through the differential activation of *t48* and *fog* across the DV axis but rather are the consequence of temporal dynamics. The first nuclei that exhibit expression are located along the ventral midline, which foreshadows the formation of the ventral furrow.

The maternal Dorsal gradient organizes DV patterning of blastoderm embryos [14, 21, 22]. It activates target genes in a concentration-dependent manner, leading to different spatial thresholds of gene activity. The advent of live imaging methods provides an opportunity to explore the temporal dynamics, not just the spatial limits, of gene activity. Conventional assays suggest that Dorsal target genes are activated prior to nc14

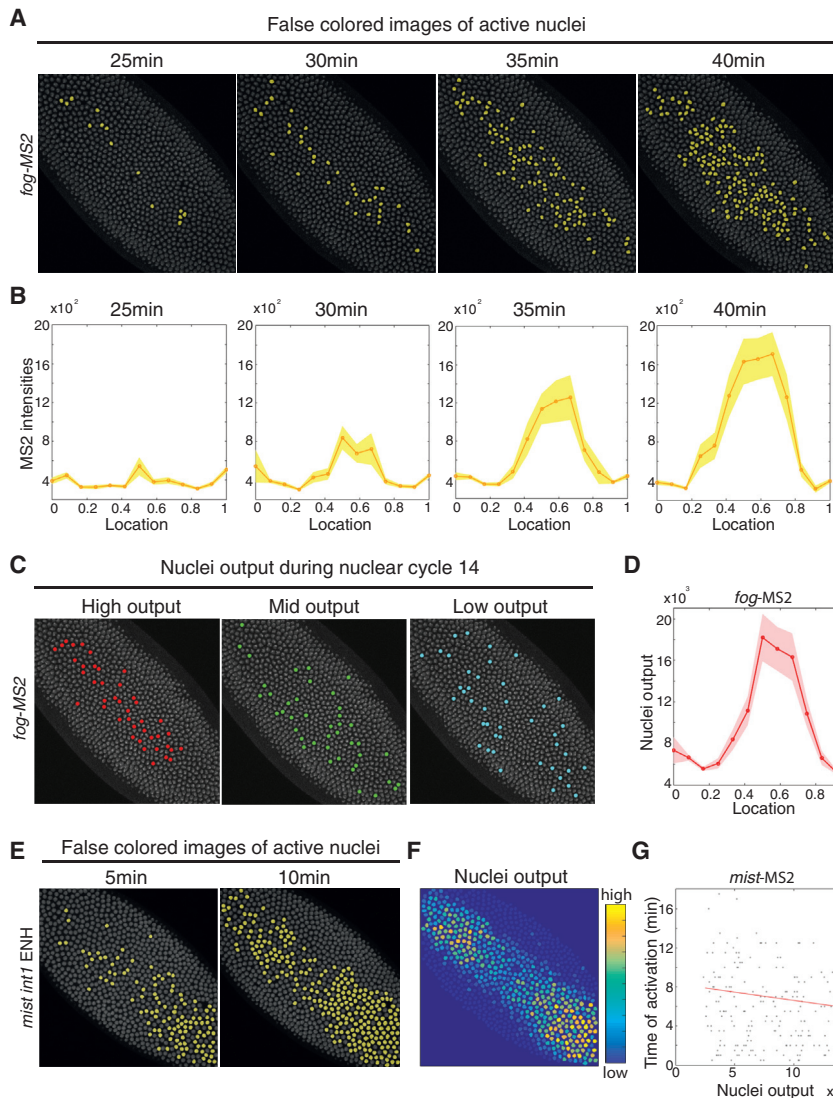


### Figure 3. Quantitative Analyses of *fog* and *mist* Transcripts during Nuclear Cycle 14

(A) Snapshots from a live imaging movie of *fog*-MS2. Actively transcribing nuclei are false colored in yellow.

(B) Mean signal intensity of *fog*-MS2 along the DV axis at each time point after the onset of nc14.

(C) Nuclei with high (90<sup>th</sup> percentile), middle (50<sup>th</sup> percentile), and low (10<sup>th</sup> percentile) output of *fog*-MS2 were labeled in red, green, and cyan, respectively.

(D) Mean cumulative outputs of *fog*-MS2 are shown along the DV axis.

(E) The false-colored snapshots of a *mist*-MS2 movie, where active nuclei are colored in yellow.

(F) Heatmap of cumulative output for the *mist*>MS2/*yellow* during nc14.

(G) Correlation between the timing of *mist*-transcriptional activation and its cumulative mRNA output over nc14. The Pearson correlation coefficient  $r = -0.41$ .

For (B) and (D), shaded area indicates the SEM of the nuclei along the same DV plane, and  $x = 0.5$  indicates the ventral midline. See also [Figures S1 and S3](#) and [Movies S2 and S3](#).

## EXPERIMENTAL PROCEDURES

### Imaging

All movies were acquired with a Zeiss LSM880 confocal microscope. A Plan-Apochromat 40 $\times$  oil immersion objective was used. 512  $\times$  512 16 bit/pixel image was obtained through bidirectional scanning mode. A stack of 30 z slices was acquired with a step size of 0.5  $\mu$ m per z slice. The time resolution was in the range of 24–30 s per entire z stacks. Three biological replicate embryos were analyzed for each transgenic line, *t48int1*>MS2, *fog*-MS2, *mistint1*>MS2, and GFP-myosin.

### Image Analysis

Segmentation, tracking, and signal measurement was performed as previously described [27], and all other analyses scripts were implemented in MATLAB. Timing of transcription activation was defined as the time point at which the MS2-*yellow* intensity becomes higher than 20% of the maximum. Cumulative mRNA output of a given nucleus was calculated by measuring the area under the transcription trajectory over time.

See also the [Supplemental Experimental Procedures](#).

## SUPPLEMENTAL INFORMATION

Supplemental Information includes Supplemental Experimental Procedures, three figures, and four movies and can be found with this article online at <http://dx.doi.org/10.1016/j.cub.2016.11.047>.

## AUTHOR CONTRIBUTIONS

Y.Y. and B.L. contributed equally. Y.Y. and M.L. designed the experiments. Y.Y. and B.L. performed the experiments and analyzed the data. Y.Y., B.L., and M.L. wrote the paper.

## ACKNOWLEDGMENTS

We are grateful to Takashi Fukaya for sharing *PCP::tdTomato* and *snail*>PP7 flies, to Adam Martin for providing GAP43-mCherry; GFP-Myosin flies, and

and sometimes display changes in expression at their boundaries [21–23]. This study provides the first evidence that the Dorsal gradient might also control the temporal dynamics of transcription.

Two-color live imaging reveals that the spatial limits of *t48* transcription are narrower than the Snail expression pattern ([Movie S4](#)), which delineates the limits of the presumptive mesoderm. We propose that the *t48* pattern delimits the region of the mesoderm that is the first to undergo apical constriction at the onset of ventral furrow formation. This is consistent with previous evidence that myosin contraction occurs in a narrower domain within the Snail expression pattern [8]. The ventral furrow has been modeled by stochastic contraction of myosin cables, superimposed on the irregular geometry of the *Drosophila* embryo [5, 24–26]. We suggest that the temporal gradients of *t48* and *fog* transcription also contribute to this process. Thus, transcriptional dynamics might be a partner of the mechanical properties of the early embryo to foster mesoderm invagination. This two-tier process is envisioned to improve the robustness of morphogenesis.

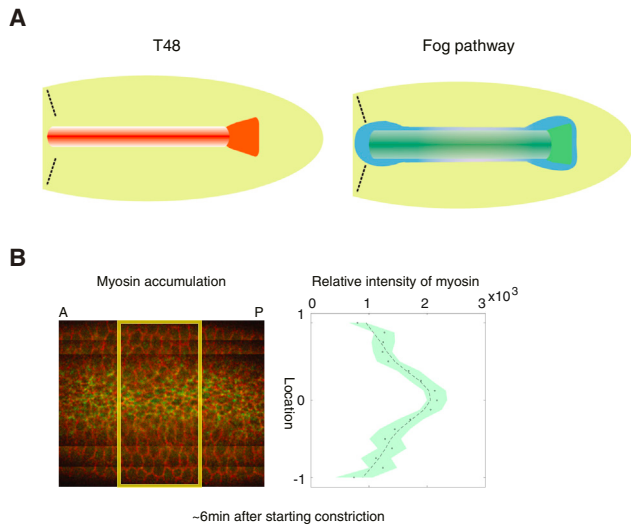


**Figure 4. Summary of *t48/fog* Pathway Activity during Mesoderm Invagination**

(A) Schematic of *t48*, *fog*, and *mist* expression patterns. *t48* (red) and *fog* (green) transcripts are spatially graded along the DV axis, whereas *mist* (blue) displays little or no gradient in activity.

(B) About 6 min after the onset of apical constriction, myosin activity is graded along the DV axis as shown in the right plot. Relative intensities of myosin in the reconstructed image were quantified, averaging the fluorescent intensities along the AP axis within the yellow square. The shaded area indicates the SEM. The dot line indicates a fitting curve.

See also [Movie S4](#).

to Thomas Gregor for providing MCP::GFP flies. We also thank Eric F. Wieschaus for helpful suggestions, as well as members of the M.L. laboratory for discussions. Y.Y. is a recipient of JSPS Overseas Research Fellowships. This study was supported by The Naito, Uehara, and Sumitomo Foundations and by a grant from the NIH to M.L. (GM46638).

Received: September 29, 2016

Revised: November 14, 2016

Accepted: November 23, 2016

Published: January 12, 2017; corrected online: February 20, 2017

## REFERENCES

- Heisenberg, C.P., and Bellaïche, Y. (2013). Forces in tissue morphogenesis and patterning. *Cell* **153**, 948–962.
- Martin, A.C., and Goldstein, B. (2014). Apical constriction: themes and variations on a cellular mechanism driving morphogenesis. *Development* **141**, 1987–1998.
- Solnica-Krezel, L., and Sepich, D.S. (2012). Gastrulation: making and shaping germ layers. *Annu. Rev. Cell Dev. Biol.* **28**, 687–717.
- Leptin, M. (1995). *Drosophila* gastrulation: from pattern formation to morphogenesis. *Annu. Rev. Cell Dev. Biol.* **11**, 189–212.
- Martin, A.C., Gelbart, M., Fernandez-Gonzalez, R., Kaschube, M., and Wieschaus, E.F. (2010). Integration of contractile forces during tissue invagination. *J. Cell Biol.* **188**, 735–749.
- Mason, F.M., Tworoger, M., and Martin, A.C. (2013). Apical domain polarization localizes actin-myosin activity to drive ratchet-like apical constriction. *Nat. Cell Biol.* **15**, 926–936.
- Kölsch, V., Seher, T., Fernandez-Ballester, G.J., Serrano, L., and Leptin, M. (2007). Control of *Drosophila* gastrulation by apical localization of adherens junctions and RhoGEF2. *Science* **315**, 384–386.
- Costa, M., Wilson, E.T., and Wieschaus, E. (1994). A putative cell signal encoded by the folded gastrulation gene coordinates cell shape changes during *Drosophila* gastrulation. *Cell* **76**, 1075–1089.
- Manning, A.J., Peters, K.A., Peifer, M., and Rogers, S.L. (2013). Regulation of epithelial morphogenesis by the G protein-coupled receptor *mist* and its ligand *fog*. *Sci. Signal.* **6**, ra98.
- Parks, S., and Wieschaus, E. (1991). The *Drosophila* gastrulation gene *concertina* encodes a G alpha-like protein. *Cell* **64**, 447–458.
- Brodland, G.W., Conte, V., Cranston, P.G., Veldhuis, J., Narasimhan, S., Hutson, M.S., Jacinto, A., Ulrich, F., Baum, B., and Miodownik, M. (2010). Video force microscopy reveals the mechanics of ventral furrow invagination in *Drosophila*. *Proc. Natl. Acad. Sci. USA* **107**, 22111–22116.
- Garcia, H.G., Tikhonov, M., Lin, A., and Gregor, T. (2013). Quantitative imaging of transcription in living *Drosophila* embryos links polymerase activity to patterning. *Curr. Biol.* **23**, 2140–2145.
- Lucas, T., Ferraro, T., Roelens, B., De Las Heras Chanes, J., Walczak, A.M., Coppey, M., and Dostatni, N. (2013). Live imaging of bicoid-dependent transcription in *Drosophila* embryos. *Curr. Biol.* **23**, 2135–2139.
- Stathopoulos, A., and Levine, M. (2002). Dorsal gradient networks in the *Drosophila* embryo. *Dev. Biol.* **246**, 57–67.
- Nien, C.Y., Liang, H.L., Butcher, S., Sun, Y., Fu, S., Gocha, T., Kirov, N., Manak, J.R., and Rushlow, C. (2011). Temporal coordination of gene networks by Zelda in the early *Drosophila* embryo. *PLoS Genet.* **7**, e1002339.
- Harrison, M.M., Li, X.Y., Kaplan, T., Botchan, M.R., and Eisen, M.B. (2011). Zelda binding in the early *Drosophila melanogaster* embryo marks regions subsequently activated at the maternal-to-zygotic transition. *PLoS Genet.* **7**, e1002266.
- Kerridge, S., Munjal, A., Philippe, J.M., Jha, A., de las Bayonas, A.G., Saurin, A.J., and Lecuit, T. (2016). Modular activation of Rho1 by GPCR signalling imparts polarized myosin II activation during morphogenesis. *Nat. Cell Biol.* **18**, 261–270.
- Gratz, S.J., Harrison, M.M., Wildonger, J., and O'Connor-Giles, K.M. (2015). Precise genome editing of *Drosophila* with CRISPR RNA-guided Cas9. *Methods Mol. Biol.* **1311**, 335–348.
- Podos, S.D., and Ferguson, E.L. (1999). Morphogen gradients: new insights from DPP. *Trends Genet.* **15**, 396–402.
- Zeller, R., López-Ríos, J., and Zuniga, A. (2009). Vertebrate limb bud development: moving towards integrative analysis of organogenesis. *Nat. Rev. Genet.* **10**, 845–858.
- Ip, Y.T., Park, R.E., Kosman, D., Bier, E., and Levine, M. (1992). The dorsal gradient morphogen regulates stripes of rhomboid expression in the presumptive neuroectoderm of the *Drosophila* embryo. *Genes Dev.* **6**, 1728–1739.
- Ip, Y.T., Park, R.E., Kosman, D., Yazdanbakhsh, K., and Levine, M. (1992). Dorsal-twist interactions establish snail expression in the presumptive mesoderm of the *Drosophila* embryo. *Genes Dev.* **6**, 1518–1530.
- Reeves, G.T., Trisnadi, N., Truong, T.V., Nahmad, M., Katz, S., and Stathopoulos, A. (2012). Dorsal-ventral gene expression in the *Drosophila* embryo reflects the dynamics and precision of the dorsal nuclear gradient. *Dev. Cell* **22**, 544–557.
- Spahn, P., and Reuter, R. (2013). A vertex model of *Drosophila* ventral furrow formation. *PLoS ONE* **8**, e75051.
- Xie, S., and Martin, A.C. (2015). Intracellular signalling and intercellular coupling coordinate heterogeneous contractile events to facilitate tissue folding. *Nat. Commun.* **6**, 7161.
- Martin, A.C., Kaschube, M., and Wieschaus, E.F. (2009). Pulsed contractions of an actin-myosin network drive apical constriction. *Nature* **457**, 495–499.
- Fukaya, T., Lim, B., and Levine, M. (2016). Enhancer control of transcriptional bursting. *Cell* **166**, 358–368.